Table 1. A summary of events during Stages I, II and III in a flash sintering experiment carried out at isothermal furnace temperature

	Furnace T.	Voltage/ Current	Time Duration	Mechanism	Initial State: powder	Initial State: Presintered Polycrystal	Electro-luminescence	Far from Equilibrium Phenomena*
Stage I	Isothermal	Voltage Control	Incubation time can vary from one second to several hours.	Joule Heating	Porous	dense polycrystal	No	No
Stage II	Isothermal	Switch from Voltage to Current Control	1–5 s	Sintering rate is four or more orders of magnitude faster than conventional	Sintering completed in about 2 s	dense polycrystal; grain growth?	Yes	?
Stage III	Furnace can be turned off	Current Control	The excited state of flash can be maintained indefinitely.	Intense Electroluminescence suggests electron hole pair formation, and electronic conductivity. Emission is NOT black body radiation.	Sample in the sintered state.	Accelerated grain growth.	Yes	Yes

*includes phase transformations, changes in the crystal structure and chemical reactions.

step produces a spike in power dissipation; this power peak is equal to the product of the applied field before the transient, and the current just afterwards. The typical switching time in our experiments is 50 ms. Under current control, generally the power dissipation declines. This combination of the rise, the peak and the decline in the power density occurs within a few seconds. We have called it Stage II. It is during this state that we note flash sintering, as shown in the bottom graph in Fig. 1. It is truly remarkable that nearly one-half of the mass is transported in the solid-state to create a dense body from a powder compact, in just a few seconds. Keep in mind that sintering requires stoichiometric mass transport, that is, chemical diffusion. Therefore, the first feature of flash sintering experiments is the colossal rate of mass transport, by some measures estimated to be four to five orders of magnitude faster than conventional diffusion.

Once the body has sintered (95% of theoretical density[4]) the sample can reside indefinitely under current control which we have called Stage III. However, this is also an abnormal state. It is an excited state of flash, where the conductivity of the sample remains high, and is "self-determined" by the material. The voltage that develops across the specimen reaches a constant value. The temperature of the specimen in this animated state also remains constant. It is fairly well explained by equating the loss from black body radiation to the electrical power expended within the sample; indeed a model based upon this axiom has been quite effective in predicting the specimen temperature.[6]

In Stage III the temperature attains a steady state for the following reason. If the temperature rises, then the resistance drops, and so does I^2R heating—the specimen cools back to its steady state temperature. If the temperature falls the resistance increases, as does the power dissipation, again restoring the steady state temperature. Thus, Stage III is a special state achieved during the flash experiment. Since it is durable, it permits detailed experiments, including in-situ experiments of X-ray diffraction at a synchrotron. The experiments can be performed only on dense sample, since sintering occurs earlier in Stage II. This article summarizes recent results from measurements in Stage III. They include electroluminescence[3] and the formation of non-equilibrium phases.[7] That is the reason this article is entitled "beyond flash sintering".

More details of the three stages of the flash sintering experiment are summarized in **Table 1**.

The remainder of this article is divided into three sections, all of them pertaining to the constant state of flash in Stage III. The first describes the specimen temperature measured by in-situ measurements of thermal expansion from shifts in the diffraction peaks. The next section summarizes measurements of electroluminescence, which are compared with black body radiation emission that would have been expected based upon the physical temperature of the specimen. Finally, we show the emergence and extinction of a non-equilibrium phase when the field is turned on and off, repeatedly.

All experiments described in this article were carried out on 3 mol % yttria stabilized zirconia (3YSZ).

2. Specimen temperature in Stage III

The specimen temperature in Stage III can be measured by in-situ X-ray diffraction from the shifts in the crystallographic peaks. Careful calibration of the thermal expansion relates the peak shifts to temperature. These experimental measurements[3] are then compared theoretical predictions from a black body radiation (BBR) model.[6]

The experimental set up used at the synchrotron at the Advanced Photon Source (APS) at Argonne National Laboratory and the Pohang Light Source II (PLS II), is shown in **Fig. 2**. More details are given in reference.[3] We use platinum as the standard to calibrate the lattice expansion of 3YSZ against temperature. A thin sliver of platinum paint is applied to a small portion of the surface of the specimen. Diffraction patterns are obtained in transmission through the entire thickness of the sample. The calibration procedure consists of heating the sample with the furnace without the application of electrical field. Well-established handbook data for thermal expansion of platinum are used to calibrate the shifts in the zirconia peak up to 1300°C, when the small amount of platinum volatilizes. This calibration is then extended up to 1600°C by extrapolating the shifts in the zirconia peak, as shown in **Fig. 3**.

In the flash experiments, the specimen temperature was increased stepwise by increasing the current. These current steps are shown in the upper graph in **Fig. 4**. The field that develops

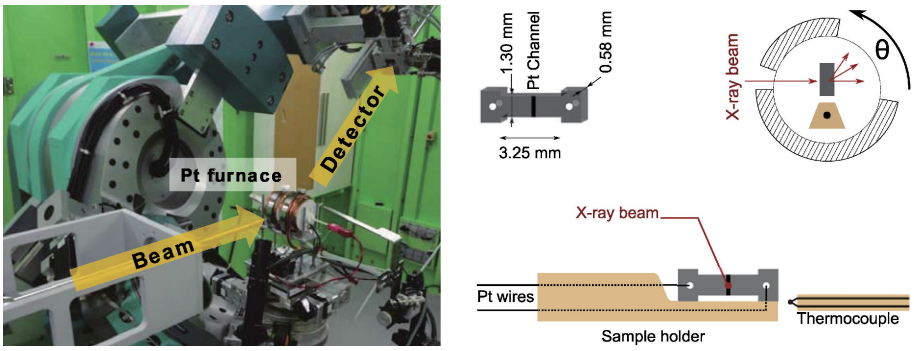

Fig. 2. The arrangement of experiments at the APS and PLS-II. The furnace was especially designed to have as small a diameter as possible in order to ensure that the temperature along the specimen was uniform to within ±3°C. The length of the hot-zone was four times the length of the specimen. Based upon.[3)]

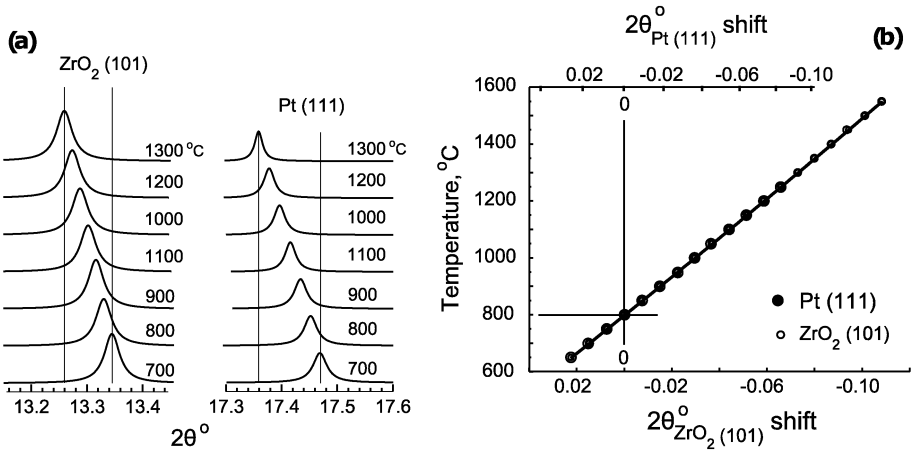

Fig. 3. The thermal expansion in zirconium oxide and in platinum is calibrated against the temperature of the furnace without the application of electric field. The Pt serves as a marker to check the calibration of thermal expansion in zirconia. (a) The peaks shift to lower Bragg angles as the temperature is raised. (b) Plots of the shifts in the peak positions against specimen temperature.[3)]

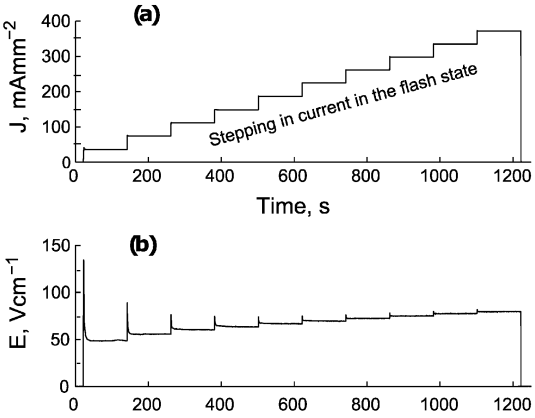

Fig. 4. (a) The specimen temperature in Stage III is raised in a stepwise fashion by raising the current. (b) The voltage that develops across the specimen under current control.[3)]

across the specimen at these current levels is given in the lower figure. The furnace temperature for these experiments was 800°C, and a field of 120 V cm^{-1} was used to initiate the flash in Stage I.

Note that the voltage does not increase in proportion to the current. That is because when the current is increased the specimen temperature rises as well. Higher specimen temperature reduces the resistance and therefore the voltage is less than that would be predicted for a constant resistance. The power density at each current level is then obtained from the product of the current that is applied and the voltage that is expressed by the sample.

Shifts in the diffraction peaks at each current are then used to measure the temperature of the specimen using the calibration curve in Fig. 3. These temperatures are plotted as a function of the power expended in the specimen in **Fig. 5**. The points are shown as dark circles, connected by a thick solid line.

The steady state temperature of the specimen can be expected to depend on the balance between the power dissipated in the specimen, which is a known quantity, and the heat lost through conduction, convention and radiation. Among these three mechanisms, the first two have a linear temperature dependence while BBR scales as the fourth power of temperature. Therefore, as a rough guide, radiation loss dominates at temperatures above 800°C. The specimen temperature can, therefore, be calculated by equating the power dissipation to black body radiation loss. Since this method does not include convection and conduction losses, this estimate of specimen temperature is an upper-bound value.

The BBR model gives the following relationship between the furnace temperature, T_F (K) the specimen temperature, T^* (K), and the specific power dissipation in the specimen, W_v expressed

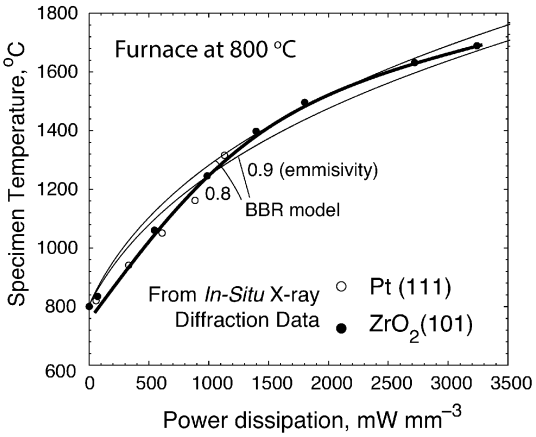

Fig. 5. Specimen temperature plotted against the power dissipation which was increased by stepping in current. The points are the temperature measurements using the calibrations in Fig. 2. The thin solid lines are the predictions from the black body radiation (BBR) model.[3),6)]

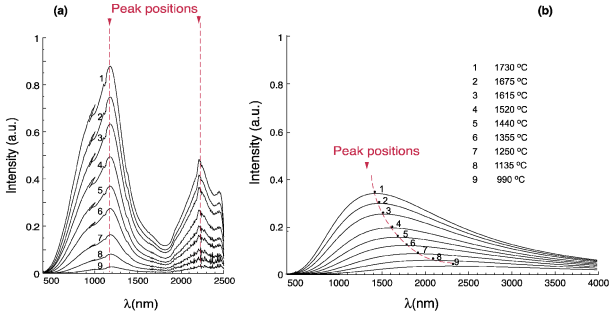

Fig. 6. (a) Electroluminescence from the specimen in Stage III. The emission intensity increases with temperature, which is a result of higher currents flowing through the specimen. Note that the position of the peaks remains unchanged. (b) Theoretical black body radiation at temperatures of the specimen reported in Fig. 5; the intensity is in arbitrary units.[3)]

in units of $mW^3\,mm^{-3}$

$$\frac{T^*}{T_F} = \left[1 + \frac{1000.W_v}{e_m \sigma T_F^4}\left(\frac{V}{A}\right)\right]^{\frac{1}{4}} \qquad (1)$$

Since heat loss depends on the surface to volume ratio of the specimen, Eq. (1) includes a factor that depends on the ratio of the volume divided by the surface area of the specimen, written as (V/A) in units of mm. e_m is the emissivity of the specimen. We assume it to lie in the 0.8–0.9 range, which is a reasonable value for oxide ceramics. The specimen temperature predicted in this way is included in Fig. 5. The estimates are in very good agreement with the experimental measurements of specimen temperature. This agreement is important since it lends credibility to the BBR model for estimating the specimen temperature, more generally.

3. Electroluminescence

With knowledge of the physical temperature of the specimen, we are now in a position to determine whether the glow emitted by the specimen is from Joule heating, or from electroluminescence. The emission spectra were measured from the visible (500 nm) into the far infrared (2500 nm), as a function of the specimen temperature, which was controlled by stepping the current flowing through the specimen, as described in the preceding section.

The emission spectra from the specimen held in the activated state of Stage III are shown in **Fig. 6**(a). The specimen temperature ranges from 990 to 1730°C. The spectra that are predicted from Joule heating (black body radiation) at the same temperatures are shown on the right in Fig. 6(b). Note that the peaks in black body radiation move to shorter wavelengths as the temperature is increased. By contrast, the experimental spectra show two distinct peaks that remain stationary but increase in intensity as the temperature rises, a behavior that is characteristic of electroluminescence that is instigated by the recombination of electrons and holes. The emission wavelength depends on the electronic structure, which is the energy levels that are occupied by the charges, while temperature determines the concentration of electrons and holes. The intensity depends on the concentration and the peak position on the energy levels.

In conclusion, the optical emission in Stage III is from electron–hole recombination and not from Joule heating.

4. Unexpected phase transformation

Further evidence that Stage III is a state that is far from equilibrium is found in the emergence of a non-equilibrium phase, which has been identified as a pseudo cubic phase[7)] of zirconia. The parent phase of the 3YSZ was tetragonal zirconia. We confirmed that the new phase was induced by the electric field, and not by Joule heating, by heating the specimen up to the same temperature that existed in Stage III, but without applying the electric field. The cubic phase for 3 mol % Yttria in zirconia is found stable only above 2100°C as suggested by phase diagram, while the lattice expansion measures the maximum specimen temperature of 1300°C under flash.[7)]

The slow emergence of the new phase when the field is on, and its gradual dissolution when the field is turned off is shown by the diffraction peak from the new phase lying midway between the diffraction peaks from (112) and (200) planes of tetragonal zirconia, in **Fig. 7**. Note how this "third peak" emerges over a period of about 10 min in Stage III, and then dissolves over a similar period when the field is turned off. The emergence and fading can be repeated over several on-off cycles. The influence of current density can be seen by comparing Figs. 7(a) and 7(b), the first at a current density of 67 mA mm^{-2} and the one on the right at 105 mA mm^{-2}. The strength of the new peak increases with current density.

The time-dependent emergence (and dissolution) of the new phase suggests that it evolves by a diffusion controlled process. Note that when the specimen is flashed again the phase appears sooner, which suggests a nucleation and growth process. The assumption being that, having been formed in a previous flash, some nuclei would have survived which start to grow more quickly when the specimen is re-flashed.

Readers may also notice a sudden shift in the peak position when the field is switched on. This is related to thermal expansion of the lattice because of joule heating,[7)] as described in section 3.

5. Discussion

The flash experiment is characterized by three stages in an experiment where the furnace is held at a constant temperature: (i) an incubation time after the application of the electric field which leads to the onset of a rapid rise in conductivity, (ii) a transient during which the power supply is switched from voltage to current control, and finally (iii) a stable state of flash under current control. This last stage, which we call Stage III, can be maintained essentially indefinitely. This is an excited state where

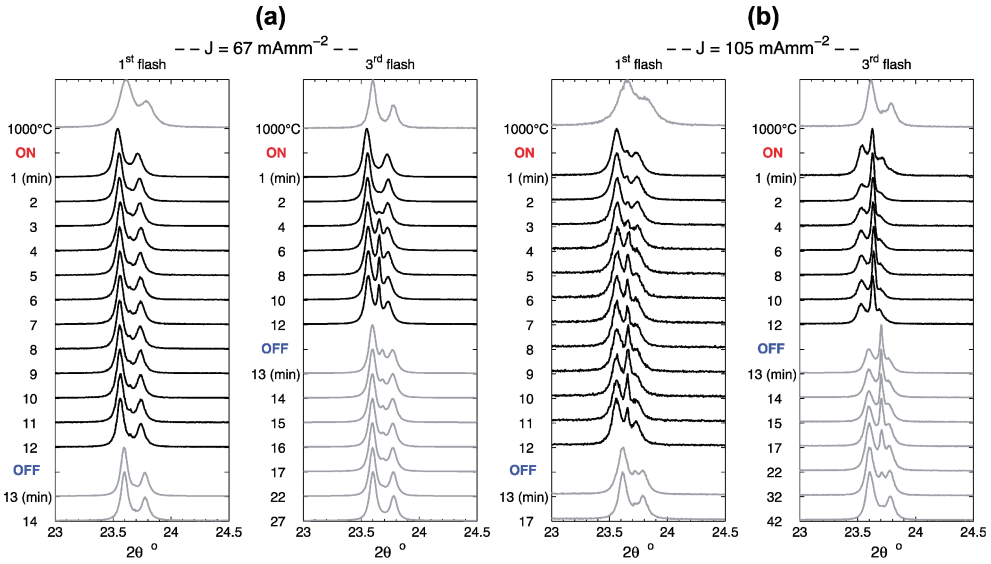

Fig. 7. Time resolved evolution and extinction of the "third peak" lying approximately midway between the (112) and (200) diffraction peaks of tetragonal zirconia. The field was left on for 12 min 30 s, and then turned off until the third peak extinguished. The samples were repeatedly flashed. Results for the 1st and a 3rd flash, at current limits of 67 and 105 mA mm^{-2}, are given.[7)]

the specimens maintains a high conductivity, electroluminesces with a green glow, and during which unusual phase transformations can occur. These peculiar phenomena are difficult to explain in terms of Joule heating and black body radiation. They are evidence of electron–hole pair generation, and the creation of charged defects that can produce non-equilibrium states when present in high concentrations.

The main question is whether or not the events in Stage III, which have been studied here, are correlated to the onset of the flash in Stage I and ultrafast sintering which occurs in Stage II. It can be stated with certainty that electroluminescence and the formation of non-equilibrium phases in Stage III cannot be attributed to Joule heating. However, the key question in the flash experiment is the cause of the first non-linearity when the current rises abruptly under voltage control. Flash sintering occurs just following that non-linearity during the period when the power supply is switched to current control (Stage II). The ultrafast sintering that occurs in Stage II certainly involves a massive increase in chemical diffusion. Whether or not that is a precursor to the defect generation in Stage III remains an open question.

Much of the discussion in recent papers has promoted Joule heating as the sole cause of the onset of the non-linearity in Stage I. The argument is that the Arrhenius increase in conductivity can produce a thermal runaway overtaking black body radiation. The result is justified from numerical analyses.[8)–10)] However, it would be wise to exercise caution: highly non-linear phenomena are usually not amenable to numerical analysis, which necessarily involve linearization of parameters as they evolve. Judgment must be exercised along the way at junctions (and singularities) where the outcomes can bifurcate towards different outcomes, which adds subjectivity to the analysis (for example, in phase transformations it has been notoriously difficult to analyze nucleation in phase transformation kinetics—it is better to use closed form expressions, even though approximate, to provide guidance in the relationship between experimental parameters and the outcome of nucleation rates[11)]). A monolithic numerical approach focused only on temperature, may miss the complexity of the

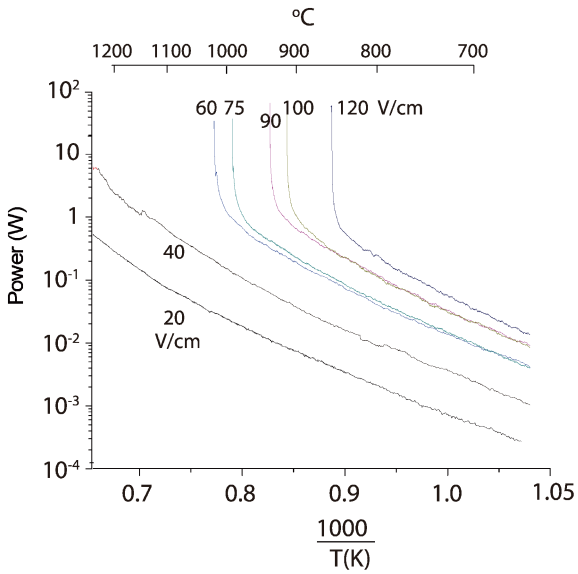

Fig. 8. The non-linear transition at the onset of flash in constant heating rate experiments at different strengths of electric fields.[1)] Note the change in behavior as the field is increased from 40 to 60 V cm^{-1}.

overall flash phenomenon, exemplified by the observations reported in this article. These observations suggest a participation by the electronic structure of the materials as well, and points towards the evolution of states that are far from equilibrium. The long incubation times in Stage I further give a glimpse into the complexity of the flash phenomena.

Nevertheless it is clear that Joule heating is important. To highlight this point we reintroduce one of the figures from the original paper,[1)] **Fig. 8**, which shows the increase in power dissipation with temperature in 3YSZ at different levels of applied field. These experiments were done at a constant heating rate of 10°C min^{-1}. Note the abrupt change in behavior as the field is increased from 40 to 60 V cm^{-1}. The transition to high conductivity occurs at about the same power level, about 1 W even

though the field increases from 60 to 120 V cm^{-1}. Conversely at lower fields the non-linearity does not occur even though power dissipation is much greater than 1 W. These graphs point towards the following inferences

(i) The stark difference in behavior at fields $\leq$40 V cm^{-1} and at fields $\geq$60 V cm^{-1}, suggests the onset of the flash, which occurs rather sharply above a critical electrical field, has a distinctly different mechanism of Joule heating above and below this transition. It is difficult to justify that Joule heating would change so dramatically over such a narrow band of experimental parameters.

(ii) It is rather remarkable that the onset of the flash always occurs at the same level of power dissipation despite different fields (60–120 V cm^{-1}) and temperatures. This phenomenological observation suggests that power dissipation and therefore Joule heating does indeed have a role in the flash mechanism.

In summary we are inclined to infer that while Joule heating is indeed a necessary condition for flash sintering, it is not sufficient to explain the various manifestations of the flash effect, which include massive chemical diffusion, electroluminescence and non-equilibrium phase transformations. Certainly observations made during Stage III suggest a role for the electronic structure and the generation of charged defects having a role in the overall process.[12] The missing link is to correlate Joule heating with the colossal generation of defects. We are far from explaining this linkage.

6. Conclusion

A flash experiment has many manifestations, a sudden increase in conductivity upon the application of an electric field, sintering in just a few seconds, and a sustained excited state under current control. The sustained state in 3YSZ is shown to emit electroluminescence (as opposed to black body radiation). The luminescence shows distinct peaks in the spectrum that reflect the difference between the energy levels of holes and electrons in the excited state, and which increase in intensity with specimen temperature. The sustained state also exhibits the emergence of non-equilibrium phases. These effects may not be explained by Joule heating alone. However, Joule heating appears to be necessary to instigate the initial onset of the flash, which is characterized by an abrupt increase in conductivity. The question of whether or not the events in Stage III, which are related to defects, are coupled in someway to what has happened before in Stages I and II, remains an open question.

Acknowledgements This work is a collaboration amongst the three authors. Lebrun and Terauds have contributed predominantly in the analysis of the X-ray data from synchrotrons, Jha has contributed predominantly in the flash experiments, and Raj in synthesizing and providing a framework for rationalizing the phenomenological information. Lebrun and Terauds are supported by a Grant No. N00014-12-1-0710 from the Office of Naval Research under the supervision of Dr. Antti Makinen and Dr. Lawrence Kabacoff. Jha and Raj are supported by a Grant from the Basic Energy Sciences Division of the Department of Energy under grant number DE-FG02-07ER46403. The Advanced Photon Source is an Office of Science User Facility operated for the U.S. Department of Energy (DOE) Office of Science by Argonne National Laboratory, supported by the U.S. DOE under Contract No. DE-AC02-06CH11357.

References

1) M. Cologna, B. Rashkova and R. Raj, *J. Am. Ceram. Soc.*, **93**, 3556–3559 (2010).
2) U. Scipioni, Electrical field assisted viscous flow in soda alumino silicate glass. M. S. Thesis, University of Trento, Trento, Italy (2011).
3) K. Terauds, J.-M. Lebrun, H.-H. Lee, T.-Y. Jeon, S.-H. Lee, J. H. Je and R. Raj, *J. Eur. Ceram. Soc.*, **35**, 3195–3199 (2015).
4) J. S. C. Francis and R. Raj, *J. Am. Ceram. Soc.*, **96**, 2754–2758 (2013).
5) K. S. Naik, V. M. Sglavo and R. Raj, *J. Eur. Ceram. Soc.*, **34**, 4063–4067 (2014).
6) R. Raj, *J. Eur. Ceram. Soc.*, **32**, 2293–2301 (2012).
7) J.-M. Lebrun, T. G. Morrissey, J. S. C. Francis, K. C. Seymour, W. M. Kriven and R. Raj, *J. Am. Ceram. Soc.*, **98**, 1493–1497 (2015).
8) R. I. Todd, E. Zapata-Solvas, R. S. Bonilla, T. Sneddon and P. R. Wilshaw, *J. Eur. Ceram. Soc.*, **33**, 2811–2816 (2013).
9) Y. Dong and I.-W. Chen, *J. Am. Ceram. Soc.*, **98**, 2333–2335 (2015).
10) S. Grasso, Y. Sakka, N. Rendtorff, C. Hu, G. Maizza, H. Borodianska and O. Vasylkiv, *J. Ceram. Soc. Japan*, **119**, 144–146 (2011).
11) D. Turnbull and J. C. Fisher, *J. Chem. Phys.*, **17**, 71–73 (1949).
12) R. Raj, M. Cologna and J. S. Francis, *J. Am. Ceram. Soc.*, **94**, 1941–1965 (2011).